Magneto−Structural Correlations in μ_2-1,1-Azide-Bridged Dicopper(II) Complexes. 2. Dominant Antiferromagnetic Coupling with Azide Bridge Angles Exceeding 108°. X-ray Structures of $[Cu_2(PAP)(\mu_2\text{-}N_3)Br_3]\cdot CH_2Cl_2$, $[Cu_2(PAP6Me)(\mu_2\text{-}N_3)(\mu_2\text{-}Br)Br_2]\cdot 1.68H_2O$, $[Cu_2(PAP6Me)(\mu_2\text{-}N_3)(\mu_2\text{-}H_2O)(NO_3)_2](NO_3)\cdot 0.75CH_3OH$, $[Cu_2(PAN)(\mu_2\text{-}N_3)(\mu_2\text{-}NO_3)(NO_3)_2]\cdot CH_3OH\cdot CH_3CN$, and $[Cu_2(PPD35Me)(\mu_2\text{-}N_3)Br_3(CH_3OH)]$

Laurence K. Thompson,* Santokh. S. Tandon, and Mike E. Manuel

Department of Chemistry, Memorial University of Newfoundland, St. John's, Newfoundland, A1B 3X7 Canada

Received October 6, 1994[⊗]

Dinuclear copper(II) complexes involving a combination of a μ_2-1,2-diazine (pyridazine or phthalazine) and a μ_2-1,1-azide bridge have been shown to exhibit net antiferromagnetism, with the azide actually contributing to total spin exchange as an antiferromagnetic bridge. X-ray structures for the complexes $[Cu_2(PAP)(\mu_2\text{-}N_3)Br_3]\cdot CH_2Cl_2$ (**1**), $[Cu_2(PAP6Me)(\mu_2\text{-}N_3)(\mu_2\text{-}Br)Br_2]\cdot 1.68H_2O$ (**3**), $[Cu_2(PAP6Me)(\mu_2\text{-}N_3)(\mu_2\text{-}H_2O)(NO_3)_2](NO_3)\cdot 0.75CH_3OH$ (**4**), $[Cu_2(PAN)(\mu_2\text{-}N_3)(\mu_2\text{-}NO_3)(NO_3)_2]CH_3OH\cdot CH_3CN$ (**5**), and $[Cu_2(PPD35Me)(\mu_2\text{-}N_3)Br_3(CH_3OH)]$ (**12**) show azide bridge angles in the range 108.7−122.5°. Compound **1** crystallized in the monoclinic system, space group $P2_1/c$, with $a = 13.390(3)$ Å, $b = 11.992(3)$ Å, $c = 16.658(2)$ Å, $\beta = 106.97(1)°$, and $Z = 4$ ($R = 0.036$, $R_w = 0.026$). Compound **3** crystallized in the monoclinic system, space group $P2_1/m$, with $a = 8.227(4)$ Å, $b = 15.719(4)$ Å, $c = 10.168(6)$ Å, $\beta = 100.89(5)°$, and $Z = 2$ ($R = 0.052$ and $R_w = 0.040$). Compound **4** crystallized in the monoclinic system, space group $P2_1/n$, with $a = 8.028(6)$ Å, $b = 16.752(7)$ Å, $c = 21.795(7)$ Å, $\beta = 95.85(5)°$, and $Z = 4$ ($R = 0.075$, $R_w = 0.062$). Compound **5** crystallized in the monoclinic system, space group $C2/c$, with $a = 18.419(4)$ Å, $b = 23.004(2))$ Å, $c = 14.545(2)$ Å, $\beta = 97.54(1)°$, and $Z = 8$ ($R = 0.070$, $R_w = 0.051$). Compound **12** crystallized in the orthorhombic system, space group *Pbca* (No. 61), with $a = 25.241(6)$ Å, $b = 14.458(3)$ Å, $c = 12.810(3)$ Å, and $Z = 8$ ($R = 0.052$, $R_w = 0.041$). Other complexes include $[Cu_2(PAP6Me)(\mu_2\text{-}N_3)Cl_3]\cdot CH_2Cl_2$ (**2**), $[Cu_2(PPD)(\mu_2\text{-}N_3)X_3]\cdot yCH_3OH\cdot zH_2O$ (X = Cl, $y = 0.5$, $z = 1.5$ (**6**); X = Br, $y = 0$, $z = 0.5$ (**7**)), $[Cu_2(PPD)(\mu_2\text{-}N_3)(N_3)_2]X$ (X = NO_3 (**8**), X = ClO_4 (**9**), X = CF_3SO_3 (**10**)), $[Cu_2(PPD35Me)(\mu_2\text{-}N_3)Cl_3]\cdot CH_3OH$ (**11**) (PAP = 1,4-bis(2′-pyridylamino)phthalazine, PAP6Me = 1,4-bis((6′-methyl-2-pyridyl)amino)phthalazine, PAN = 1,4-bis(2-pyridylamino)naphthalazine, PPD = 3,6-bis(1-pyrazolyl)-pyridazine, PPD35Me = 3,6-bis(3-dimethyl-1-pyrazolyl)pyridazine). Very strong net antiferromagnetic coupling is observed for **6**−**12**, which have large azide bridge angles ($-2J > 780$ cm^{-1}), while compounds **1**−**5** have much smaller azide bridge angles and exhibit much weaker net antiferromagnetism. In all cases, both azide and diazine appear to be acting in a complementary manner with both parallel, magnetically active bridge groups (N_3, diazine), contributing to total exchange in an antiferromagnetic sense. The new structurally characterized complexes provide additional support for the antiferromagnetic realm of the μ_2-1,1-azide bridge at azide bridge angles exceeding 108°.

Introduction

Considerable knowledge has been gained in understanding the magneto−structural relationships in symmetrical dibridged dinuclear metal complexes, in particular the dihydroxo-bridged copper(II) complexes studied by Hatfield et al.,[1] where a good linear relationship between exchange integral and hydroxide bridge angle was demonstrated in the range 95−105°. The practical point of *accidental orthogonality* in this series of compounds occurred at $\Phi_0 \approx 97.5°$, some 5.5° higher than the value calculated for a simple dihydroxy-bridged dicopper(II) species $[(NH_3)_2Cu(\mu_2\text{-}OH)_2Cu(NH_3)_2]^{2+}$, using extended Hückel calculations (92°) (assuming reasonable sp hybridization).[2] For a less electronegative bridge group, e.g. azide in $[(NH_3)_2Cu(\mu_2\text{-}1,1\text{-}N_3)_2Cu(NH_3)_2]^{2+}$, the calculated angle for *accidental orthogonality* occurs at 103°,[2] and so one might anticipate the practical value for Φ_0 to be somewhat higher. Earlier studies on two symmetric di-μ_2-1,1-azide-bridged dicopper(II) complexes with bridge angles in the range 100.5(6)−105.46(9)°[3,4] revealed strong ferromagnetic coupling between the copper centers, propagated by the azide bridges, essentially in agreement with theoretical calculations.[2] No studies have been reported so far on a series of di-μ_2-1,1-azide-bridged complexes with varying azide bridge angles, similar to the dihydroxy bridged series, which might reveal the predicted antiferromagnetic nature of the azide bridge at large bridge angles. The creation of large azide bridge angles without additional ligand control would be difficult. We recently[5] showed that, by the use of tetradentate, dinucleating diazine ligands, with controllable bite, we were able to create μ_2-1,1-azide-bridged dicopper(II) complexes with

* Author to whom correspondence should be addressed.

[⊗] Abstract published in *Advance ACS Abstracts,* April 1, 1995.

(1) Crawford, V. H.; Richardson, H. W.; Wasson, J. R.; Hodgson, D. J.; Hatfield, W. E. *Inorg. Chem.* **1976**, *15*, 2107.
(2) Kahn, O. *Inorg. Chim. Acta* **1982**, *62*, 3.
(3) Sikorav, S.; Bkouche-Waksman, I.; Kahn, O. *Inorg. Chem.* **1984**, *23*, 490.
(4) Comarmond, J.; Plumeré, P.; Lehn, J.-M.; Agnus, Y.; Louis, R.; Weiss, R.; Kahn, O.; Morgenstern-Badarau, I. *J. Am. Chem. Soc.* **1982**, *104*, 6330.
(5) Tandon, S. S.; Thompson, L. K.; Manuel, M. E.; Bridson, J. N. *Inorg. Chem.* **1994**, *33*, 5555.

0020-1669/95/1334-2356$09.00/0

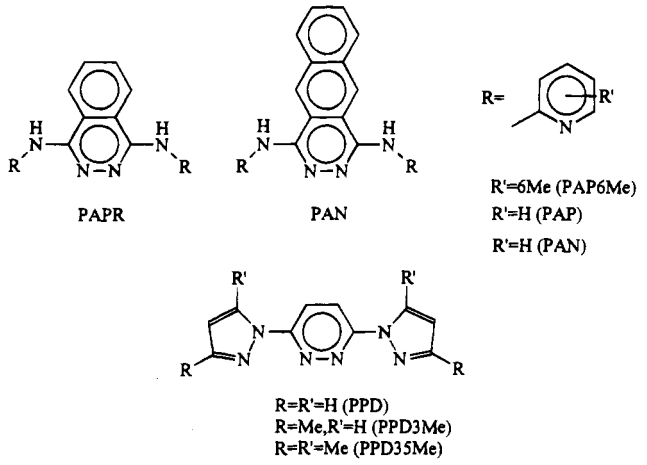

Figure 1. Tetradentate diazine ligands.

bridge angles in the range 98.3−124.1°, more than enough to cover the anticipated angle for *accidental orthogonality*, which was found to occur at ≈108.5°.[5] These complexes are mostly asymmetric, dibridged systems, with a diazine (pyridazine, phthalazine, or thiadiazole) and an azide bridge linking two $d_{x^2-y^2}$ copper(II) centers, and parallel a series of asymmetric, dinuclear copper(II) complexes involving a diazine (phthalazine or pyridazine) and a hydroxide as equatorial magnetic bridges ($d_{x^2-y^2}$ copper), in which a linear relationship between exchange integral and hydroxide bridge angle was demonstrated (Cu−OH−Cu 100−116°).[6] Exchange integrals ($2J$) were found to vary from −150 to −1300 cm^{-1} for the hydroxide-bridged complexes[6] and from +170 to −1100 cm^{-1} for the azide-bridged complexes,[5] with comparable ligands. At large bridge angles in both series it is clear that the exchange process is dominated by the hydroxide or azide bridge. For the hydroxide-bridged complexes the available angles are all > Φ_0, beyond its ferromagnetic realm, and so the overall exchange process in these systems is the result of two contributing and complementary antiferromagnetic pathways. For the azide-bridged complexes at small bridge angles (<≈108°) the ferromagnetic coupling associated with the azide more than compensates for the antiferromagnetic effect of the diazine bridge and the systems exhibit net ferromagnetism. At larger bridge angles net antiferromagnetism is observed and the azide bridge exhibits an antiferromagnetic effect.[5]

This paper describes a number of additional examples of diazine/μ_2-1,1-azide-dibridged dicopper(II) complexes, involving 6,6,6 and 5,6,5 ligands (see structure **I** and Figure 1), all

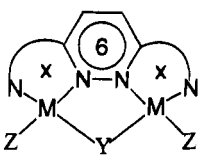

I

exhibiting net antiferromagnetism, with $-2J$ in the range 112−932 cm^{-1}. The structurally characterized complexes (**1**, **3**−**5**, **12**) have azide bridge angles in the range 108.7−122.5° and provide additional examples that reinforce the established trend for this bridge, involving the change from ferromagnetic to antiferromagnetic behavior at angles >≈108°.[5] A quantitative correlation between exchange integral and azide bridge angle is established.

(6) Thompson, L. K.; Lee, F. L.; Gabe, E., J. *Inorg. Chem.* **1988**, *27*, 39.

Experimental Section

The ligands PAP,[7] PAP6Me,[8] PPD,[9] and PPD35Me[9] were prepared by published procedures. PAN was prepared using a procedure similar to the synthesis of PAP6Me[8] using 2,3-naphthalenedicarbonitrile.[10]

$Cu_2(PAP)(\mu_2\text{-}N_3)Br_3]\cdot CH_2Cl_2$ (1). A solution of $CuBr_2$ (0.300 g, 1.3 mmol) in hot CH_3OH (20 mL) was added to a solution of PAP (0.100 g, 0.32 mmol) in hot CH_2Cl_2 (20 mL). NaN_3 (0.05 g, 0.77 mmol) dissolved in hot CH_3OH (10 mL) was added immediately and the green solution allowed to stand. Green crystals formed, which were filtered off, washed with CH_3OH, and air-dried. Yield: 0.13 g. **2** and **3** were prepared in a similar manner. Anal. Calcd for $[Cu_2(C_{18}H_{14}N_6)(N_3)Br_3]\cdot CH_2Cl_2$ (**1**): C, 28.24; H, 2.00; N, 15.60. Found: C, 28.49; H, 2.36; N, 15.72. Calcd for $[Cu_2(C_{20}H_{18}N_6)(N_3)Cl_3]\cdot CH_2Cl_2$ (**2**): C, 35.89; H, 2.30; N, 17.94. Found: C, 35.92; H, 2.92; N, 17.78. Calcd for $[Cu_2(C_{20}H_{18}N_6)(N_3)Br_3]\cdot 0.5CH_3OH$ (**3**): C, 32.09; H, 2.63; N, 16.43. Found: C, 32.45; H, 2.89; N, 16.60. The sample of **3** prepared for structural analysis was found to have lattice water, rather than methanol. Variable-temperature magnetism was done on this sample.

$[Cu_2(PAP6Me)(\mu_2\text{-}N_3)(\mu_2\text{-}H_2O)(NO_3)_2](NO_3)$ (4). $Cu(NO_3)_2.3H_2O$ (0.350 g, 1.45 mmol) dissolved in hot CH_3OH (30 mL) was added to a solution of PAP6Me (0.050 g, 0.15 mmol) in hot CH_2Cl_2 (20 mL), and the mixture was heated on a steam bath for 2−3 min. NaN_3 (0.030g, 0.46 mmol) dissolved in hot CH_3OH (10 mL) was added and the mixture heated 2−3 min more and filtered hot, and the filtrate was allowed to stand. Green crystals formed after several days, which were filtered off, washed with CH_3OH (2 × 2 mL), and dried under vacuum. Yield: 0.025 g. Anal. Calcd for $[Cu_2(C_{20}H_{18}N_6)(N_3)(NO_3)_2](NO_3)$: C, 34.44; H, 2.60; N, 23.89: Found: C, 34.22; H, 2.35; N, 23.89. The sample used for structural analysis was air-dried and found to contain methanol solvate.

$[Cu_2(PAN)(\mu_2\text{-}N_3)(\mu_2\text{-}NO_3)(NO_3)_2]\cdot CH_3OH\cdot CH_3CN\cdot 4.5H_2O$ (5). PAN (0.050 g, 0.14 mmol) was dissolved in a CH_3CN/CH_3OH mixture (20 mL/55 mL), and the solution was added to a solution of $Cu(NO_3)_2\cdot 3H_2O$ (0.066 g, 0.36 mmol) in CH_3CN (15 mL). A solution of NaN_3 (0.008 g, 0.13 mmol) in CH_3OH (5 mL) was added quickly, with the formation of a dark green solution. Green crystals formed on standing. Yield: 20 mg. Anal. Calcd for $[Cu_2(C_{22}H_{16}N_6)(N_3)(NO_3)_3]\cdot CH_3OH\cdot CH_3CN\cdot 4.5H_2O$: C, 34.37; H, 3.66; N, 20.84. Found: C, 34.18; H, 2.87; N, 20.72.

$[Cu_2(PPD)(\mu_2\text{-}N_3)(N_3)_2](ClO_4)$ (9). PPD (0.100 g, 0.47 mmol) dissolved in hot CH_3CN (20 mL) was added to a solution of $Cu(ClO_4)\cdot 6H_2O$ (0.400 g, 1.1 mmol) in hot CH_3OH (15 mL), and the mixture was warmed for ≈1 min. A solution of NaN_3 (0.060g, 0.92 mmol) in H_2O (10 mL) was added dropwise and the mixture shaken, forming a dark green solution. A small amount of brown precipitate was filtered off and discarded, and the filtrate was allowed to stand. Dark green crystals formed, which were washed with CH_3OH and dried under vacuum. Yield: 0.050 g. **6**−**8** and **10** were prepared in a similar manner. Anal. Calcd for $[Cu_2(C_{10}H_8N_6)(N_3)_3](ClO_4)$ (**9**): C, 21.27; H, 1.43: N, 37.20. Found: C, 21.21; H, 1.78; N, 37.75. Calcd for $[Cu_2(C_{10}H_8N_6)(N_3)Cl_3]\cdot 0.5CH_3OH\cdot 1.5H_2O$ (**6**): C, 23.76; H, 2.45; N, 23.75. Found: C, 23.84; H, 2.15; N, 23.71. Calcd for $[Cu_2(C_{10}H_8N_6)(N_3)Br_3]\cdot 0.5H_2O$ (**7**): C, 18.93; H, 1.51; N, 19.87. Found: C, 18.92; H, 1.61; N, 19.97. Calcd for $[Cu_2(C_{10}H_8N_6)(N_3)_3](NO_3)\cdot 0.5H_2O$ (**8**): C, 22.39; H, 1.69; N, 41.78. Found: C, 22.29; H, 1.90; N, 41.75. Calcd for $[Cu_2(C_{10}H_8N_6)(N_3)_3](CF_3SO_3)\cdot 0.5CH_3OH$ (**10**): C, 21.90; H, 1.59; N, 33.33. Found: C, 21.87; H, 1.55; N, 33.48.

$[Cu_2(PPD35Me)(\mu_2\text{-}N_3)Cl_3]\cdot CH_3OH$ (11). PPD35Me (0.100 g, 0.37 mmol) was dissolved in hot CH_3CN (15 mL) and added to a solution of $CuCl_2\cdot 2H_2O$ (0.200 g, 1.2 mmol) in hot CH_3OH (15 mL). The mixture was warmed for ≈1 min and a solution of NaN_3 (0.025 g, 0.38 mmol) in CH_3OH (5 mL) added dropwise with shaking. The dark green solution was filtered, and the filtrate was allowed to stand

(7) Thompson, L. K.; Chacko, V. T.; Elvidge, J. A.; Lever, A. B. P.; Parish, R. V. *Can. J. Chem.* **1969**, *47*, 4141.
(8) Bautista, D. V.; Bullock, G.; Hartstock, F. W.; Thompson, L. K. *J. Heterocycl. Chem.* **1983**, *20*, 345.
(9) Thompson, L. K.; Woon, T. C.; Murphy, D. B.; Gabe, E. J.; Lee, F. L.; Le Page, Y. *Inorg. Chem.* **1985**, *24*, 4719.
(10) Kovshev, E. I.; Puchnova, V. A.; Luk'yanets, E. A. *J. Org. Chem. USSR (Engl. Transl.)* **1971**, *7*, 364.

Table 1. Summary of Crystallographic Data for $[Cu_2(PAP)(\mu_2\text{-}N_3)Br_3]\cdot CH_2Cl_2$ (**1**), $[Cu_2(PAP6Me)(\mu_2\text{-}N_3)(\mu_2\text{-}Br)Br_2]\cdot 1.68H_2O$ (**3**), $[Cu_2(PAP6Me)(\mu_2\text{-}N_3)(\mu_2\text{-}H_2O)(NO_3)_2](NO_3)\cdot 0.75CH_3OH$ (**4**), $[Cu_2(PAN)(\mu_2\text{-}N_3)(\mu_2\text{-}NO_3)(NO_3)_2]\cdot CH_3OH\cdot CH_3CN$ (**5**), and $[Cu_2(C_{14}H_{16}N_6)(N_3)Br_3(CH_3OH)]$ (**12**)

	1	**3**	**4**	**5**	**12**
empirical formula	$C_{19}H_{16}N_9Br_3Cl_2Cu_2$	$C_{20}H_{21.37}N_9Br_3O_{1.68}Cu_2$	$C_{20.75}H_{23}N_{12}O_{10.75}Cu_2$	$C_{25}H_{23}N_{13}O_{13}Cu_2$	$C_{15}H_{20}N_9Br_3OCu_2$
fw	808.11	781.50	739.58	792.63	709.19
space group	$P2_1/c$	$P2_1/m$	$P2_1/n$	$C2/c$	*Pbca* (No. 61)
a (Å)	13.390(3)	8.227(4)	8.028(6)	18.419(4)	25.241(6)
b (Å)	11.992(3)	15.719(4)	16.752(7)	23.004(2)	14.458(3)
c (Å)	16.658(2)	10.168(6)	21.795(7)	14.545(2)	12.810(3)
α (deg)					
β (deg)	106.97(1)	100.89(5)	95.85(5)	97.54(1)	
γ (deg)					
V (Å^3)	2558(1)	1291(1)	2916(2)	6110(2)	4675(4)
ϱ_{calcd} (g cm^{-3})	2.098	2.010	1.685	1.723	2.015
Z	4	2	4	8	8
μ (cm^{-1})	65.49	62.85	15.36	14.71	69.32
λ (Å)	0710 69	0.710 69	0.710 69	0.710 69	0.710 69
T (°C)	26	26	26	26	26
R^a	0.036	0.052	0.075	0.070	0.052
$R_w{}^b$	0.026	0.040	0.062	0.051	0.041

$^a R = \sum||F_o| - |F_c||/\sum|F_o|$. $^b R_w = [(\sum w(|F_o| - |F_c|)^2/\sum wF_o^2)]^{1/2}$.

overnight. Dark green crystals formed, which were filtered off, washed with CH_3OH/CH_3CN (1:1) (3 × 3 mL), and dried under vacuum. Yield: 0.14 g. **12** was prepared in a similar manner. Anal. Calcd for $[Cu_2(C_{14}H_{16}N_6)(N_3)Cl_3]\cdot CH_3OH$ (**11**): C, 31.29; H, 3.50; N, 21.90. Found: C, 31.22; H, 3.38; N, 22.06. Calcd for $[Cu_2(C_{14}H_{16}N_6)(N_3)Br_3]\cdot 0.6CH_3OH$ (**12**): C, 25.18; H, 2.64; N, 18.10. Found: C, 24.90; H, 2.61; N, 17.88.

The X-ray sample of **12** was shown to contain one coordinated methanol.

Physical Measurements. Electronic spectra were recorded as Nujol mulls using a Cary 5E spectrometer. Infrared spectra were recorded as Nujol mulls using a Mattson Polaris FT-IR instrument. Microanalyses were carried out by the Canadian Microanalytical Service, Delta, Canada. Room-temperature magnetic susceptibilities were measured by the Faraday method using a Cahn 7600 Faraday magnetic balance, and variable-temperature magnetic data (4−300 K) were obtained using an Oxford Instruments superconducting Faraday susceptometer with a Sartorius 4432 microbalance. A main solenoid field of 1.5 T and a gradient field of 10 T m^{-1} were employed.

Safety Note. Azide compounds are potentially explosive and should be treated with care and in small quantities. In particular, copper(II) azide is explosive, and in those reactions where an excess of copper(II) salt is used, followed by addition of azide, an excess of azide should be avoided. A small explosion resulted when a small quantity of a solid azide complex, which was synthesized in this way, was handled. This was attributed to copper azide impurity. Most of the complexes reported here were synthesized by adding limited amounts of sodium azide and did not produce explosive material.

Crystallographic Data Collection and Refinement of the Structures. $[Cu_2(PAP)(\mu_2\text{-}N_3)Br_3]\cdot CH_2Cl_2$ (1). The crystals of **1** are dark green, almost black in appearance. The diffraction intensities of an approximately 0.30 × 0.20 × 0.15 mm crystal were collected with graphite-monochromatized Mo Kα radiation using a Rigaku AFC6S diffractometer at 26 ± 1 °C and the $\omega-2\theta$ scan technique to a $2\theta_{max}$ value of 50.1°. A total of 4990 reflections were measured, of which 4777 (R_{int} =0.041) were unique and 2762 were considered significant with $I_{net} > 2.0\sigma(I_{net})$. An empirical absorption correction was applied, after a full isotropic refinement, using the program DIFABS,[11] which resulted in transmission factors ranging from 0.84 to 1.00. The data were corrected for Lorentz and polarization effects. The cell parameters were obtained from the least-squares refinement of the setting angles of 25 carefully centered reflections with 2θ in the range 20.43−40.22°.

The structure was solved by direct methods.[12,13] All atoms except hydrogens were refined anisotropically. Hydrogen atoms were included in calculated positions with isotropic thermal parameters set 20% greater than those of their bonded partners. Hydrogens were included, but not refined, in the final rounds of least-squares. The final cycle of full-matrix least-squares refinement was based on 2762 observed reflections ($I > 2.00\sigma(I)$) and 316 variable parameters and converged with unweighted and weighted agreement factors of $R = \sum||F_o| - |F_c||/\sum|F_o| = 0.036$ and $R_w = [(\sum w(|F_o| - |F_c|)^2/\sum wF_o^2)]^{1/2} = 0.026$. The maximum and minimum peaks on the final difference Fourier map correspond to 0.49 and - 0.48 electron/Å^3, respectively. Neutral-atom scattering factors[14] and anomalous-dispersion terms[15,16] were taken from the usual sources. All calculations were performed with the TEXSAN[17] crystallographic software package using a VAX 3100 work station. A summary of the crystal and other data is given in Table 1, and atomic coordinates are given in Table 2. Hydrogen atom coordinates (Table S1), anisotropic thermal parameters (Table S2), a full listing of bond distances and angles (Table S3), and least squares planes data (Table S4) are included as supplementary material.

$[Cu_2(PAP6Me)(\mu_2\text{-}N_3)(\mu_2\text{-}Br)Br_2]\cdot 1.68H_2O$ (3). The diffraction intensities of a dark brown crystal of approximate dimensions 0.40 × 0.20 × 0.20 mm were collected on a Rigaku AFC6S diffractometer in a fashion similar to that used for **1.** Hydrogen atoms were placed in calculated positions with isotropic thermal parameters set 20% greater than those of their bonded partners. A partially occupied, diffuse water molecule was included at two sites (occupancy 0.84). A summary of crystal and other data is given in Table 1, and atomic coordinates are given in Table 3. Hydrogen atom coordinates (Table S5), anisotropic thermal parameters (Table S6), a full listing of bond distances and angles (Table S7), and least-squares planes (Table S8) are included as supplementary material.

$[Cu_2(PAP6Me)(\mu_2\text{-}N_3)(\mu_2\text{-}H_2O)(NO_3)_2](NO_3)\cdot 0.75CH_3OH$ (4). The diffraction intensities of a dark green hexagonal columnar crystal of approximate dimensions 0.40 × 0.20 × 0.15 mm were collected on a Rigaku AFC6S diffractometer in a fashion similar to that used for **1.** Hydrogen atoms were placed in calculated positions with isotropic thermal parameters set 20% greater than those of their bonded partners. A partially occupied methanol molecule (75% occupancy) was found in the lattice. A summary of crystal and other data is given in Table 1, and atomic coordinates are given in Table 4. Hydrogen atom coordinates (Table S9), anisotropic thermal parameters (Table S10), a full listing of bond distances and angles (Table S11), and least-squares planes (Table S12) are included as supplementary material.

$[Cu_2(PAN)(\mu_2\text{-}N_3)(\mu_2\text{-}NO_3)(NO_3)_2]\cdot CH_3OH\cdot CH_3CN$ (5). The diffraction intensities of a green, irregular crystal of approximate dimen-

(11) Walker, N.; Stuart, D. *Acta Crystallogr.* **1983**, *A39*, 158.
(12) Gilmore, C. J. *J. Appl. Crystallogr.* **1984**, *17*, 42.
(13) Beurskens, P. T. DIRDIF. Technical Report 1984/1; Crystallography Laboratory: Toernooiveld, 6525 Ed Nijmegen, The Netherlands, 1984.
(14) Cromer, D. T.; Waber, J. T. *International Tables for X-ray Crystallography*; The Kynoch Press: Birmingham, U.K., 1974; Vol. IV, Table 2.2A.
(15) Ibers, J. A.; Hamilton, W. C. *Acta Crystallogr.* **1974**, *17*, 781.
(16) Cromer, D. T. *International Tables for X-ray Crystallography*; The Kynoch Press: Birmingham, U.K., 1974; Vol. IV, Table 2.3.1.
(17) *Texsan-Texray Structure Analysis Package*; Molecular Structure Corp.: The Woodlands, TX, 1985.

Table 2. Final Atomic Positional Parameters and B(eq) Values (Å^2) for $[Cu_2(PAP)(\mu_2\text{-}N_3)Br_3]\cdot CH_2Cl_2$ (**1**)

atom	x	y	z	B(eq)[a]
Br(1)	0.20290(5)	0.11703(6)	0.68264(4)	2.94(3)
Br(2)	0.29082(6)	0.34283(6)	0.54531(4)	3.43(3)
Br(3)	0.57172(5)	0.12021(7)	0.57134(4)	3.18(3)
Cu(1)	0.19543(6)	0.14872(7)	0.53681(4)	2.20(3)
Cu(2)	0.39923(6)	0.14814(7)	0.47670(5)	2.65(4)
Cl(1)	0.7027(2)	0.0418(2)	0.1068(1)	5.6(1)
Cl(2)	0.7839(2)	0.2127(2)	0.2330(1)	7.4(1)
N(1)	0.0451(4)	0.1914(4)	0.5065(3)	2.0(2)
N(2)	−0.0010(4)	0.0720(5)	0.3888(3)	2.7(2)
N(3)	0.1731(3)	0.1180(4)	0.4127(3)	2.1(2)
N(4)	0.2603(3)	0.1339(4)	0.3862(3)	2.1(2)
N(5)	0.3392(4)	0.1401(5)	0.2793(3)	2.3(2)
N(6)	0.4445(4)	0.2402(4)	0.3955(3)	2.4(2)
N(7)	0.3301(4)	0.0748(5)	0.5494(3)	2.6(3)
N(8)	0.3676(4)	0.0039(5)	0.6013(4)	2.7(3)
N(9)	0.4021(5)	−0.0624(6)	0.6497(4)	5.0(4)
C(1)	0.0129(5)	0.2592(6)	0.5600(4)	3.1(3)
C(2)	−0.0897(6)	0.2672(7)	0.5592(5)	3.8(4)
C(3)	−0.1632(5)	0.2057(6)	0.5028(4)	3.5(3)
C(4)	−0.1332(5)	0.1424(6)	0.4458(4)	3.0(3)
C(5)	−0.0280(5)	0.1368(6)	0.4493(4)	2.4(3)
C(6)	0.0869(5)	0.0769(5)	0.3625(4)	2.0(3)
C(7)	0.0815(5)	0.0346(5)	0.2796(4)	2.2(3)
C(8)	−0.0051(5)	−0.0198(6)	0.2265(4)	3.5(4)
C(9)	−0.0013(6)	−0.0615(6)	0.1513(4)	4.0(4)
C(10)	0.0882(6)	−0.0525(6)	0.1271(4)	3.6(4)
C(11)	0.1736(5)	0.0020(6)	0.1769(4)	2.8(3)
C(12)	0.1703(5)	0.0474(5)	0.2533(4)	2.0(3)
C(13)	0.2576(4)	0.1095(5)	0.3087(4)	2.0(3)
C(14)	0.4157(4)	0.2214(5)	0.3128(4)	2.1(3)
C(15)	0.4604(5)	0.2782(6)	0.2587(4)	2.9(3)
C(16)	0.5321(5)	0.3578(7)	0.2910(4)	3.8(4)
C(17)	0.5592(5)	0.3834(6)	0.3755(4)	4.0(4)
C(18)	0.5146(5)	0.3224(6)	0.4253(4)	3.4(3)
C(19)	0.6778(6)	0.1256(7)	0.1842(5)	5.3(4)

[a] $B(\text{eq}) = (8\pi^2/3)\sum_{i=1}^{3}\sum_{j=1}^{3}U_{ij}\boldsymbol{a}_i^*\boldsymbol{a}_j^*\vec{a}_i\vec{a}_j$.

Table 3. Final Atomic Positional Parameters and B(eq) Values (Å^2) for $[Cu_2(PAP6Me)(\mu_2\text{-}N_3)(\mu_2\text{-}Br)Br_2]\cdot 1.68H_2O$ (**3**)

atom	x	y	z	B(eq)[a]
Br(1)	0.7150(3)	1/4	0.9342(2)	3.8(1)
Br(2)	0.9249(2)	0.0619(1)	0.6564(2)	4.18(8)
Cu(1)	0.7017(2)	0.1481(1)	0.7120(2)	2.77(7)
N(1)	0.569(1)	0.0490(6)	0.753(1)	2.7(5)
N(2)	0.364(1)	0.0769(6)	0.557(1)	2.6(5)
N(3)	0.485(1)	0.2067(5)	0.6265(9)	2.4(4)
N(4)	0.809(2)	1/4	0.662(2)	3.7(4)
N(5)	0.823(2)	1/4	0.545(3)	7.6(6)
N(6)	0.844(3)	1/4	0.432(3)	12.5(9)
C(1)	0.776(2)	0.0188(8)	0.952(1)	4.3(7)
C(2)	0.625(1)	−0.0063(8)	0.858(1)	2.6(6)
C(3)	0.541(2)	−0.0788(9)	0.871(1)	4.3(8)
C(4)	0.407(2)	−0.1046(9)	0.782(1)	4.2(7)
C(5)	0.346(2)	−0.0490(7)	0.680(1)	3.2(6)
C(6)	0.429(2)	0.0253(8)	0.668(1)	2.9(6)
C(7)	0.373(1)	0.1625(8)	0.544(1)	2.8(6)
C(8)	0.265(1)	0.2061(7)	0.434(1)	2.7(6)
C(9)	0.171(2)	0.1619(8)	0.327(1)	3.6(6)
C(10)	0.077(2)	0.2063(7)	0.224(1)	4.2(7)
O(1)	0.185(8)	1/4	0.8136	23(2)
O(2)	0.23(1)	1/4	0.88(1)	34(2)

[a] $B(\text{eq}) = (8\pi^2/3)\sum_{i=1}^{3}\sum_{j=1}^{3}U_{ij}\boldsymbol{a}_i^*\boldsymbol{a}_j^*\vec{a}_i\vec{a}_j$.

sions 0.40 × 0.20 × 0.10 mm were collected on a Rigaku AFC6S diffractometer in a manner similar to that used for **1**. Fairly extensive crystal decomposition occurred in the X-ray beam, and the intensities of three representative reflections decayed by −54% during data collection. A linear absorption correction was applied to account for this. A loosely bound nitrate occurs as a pseudoaxial bridging group. A well-defined acetonitrile molecule appears in the lattice, and an additional solvent cluster, close to a special position, has been interpreted as a methanol molecule, in agreement with elemental analytical data. Hydrogen atoms were included in calculated positions, with isotropic thermal parameters set 20% greater than those of their bonded partners. A summary of crystal and other data is given in Table 1, and atomic coordinates are given in Table 5. Hydrogen atom coordinates (Table S13), anisotropic thermal parameters (Table S14), a full listing of bond distances and angles (Table S15), and least-squares planes data (Table S16) are included as supplementary data.

Table 4. Final Atomic Positional Parameters and B(eq) Values (Å^2) for $[Cu_2(PAP6Me)(\mu_2\text{-}N_3)(\mu_2\text{-}H_2O)(NO_3)_2](NO_3)\cdot 0.75CH_3OH$ (**4**)

atom	x	y	z	B(eq)[a]
Cu(1)	0.3033(2)	0.1029(1)	0.69886(8)	3.00(8)
Cu(2)	0.3545(2)	0.2453(1)	0.60356(8)	3.17(8)
O(1)	0.094(1)	0.0893(7)	0.7387(4)	4.4(6)
O(2)	−0.138(1)	0.019(1)	0.7220(6)	10(1)
O(3)	0.069(2)	0.0024(7)	0.6666(6)	7.3(8)
O(4)	0.184(1)	0.3227(9)	0.5742(6)	8.6(9)
O(5)	0.127(2)	0.4012(8)	0.4934(6)	8.2(8)
O(6)	0.239(2)	0.282(1)	0.4895(8)	14(1)
O(7)	0.621(2)	0.1868(6)	0.3864(5)	6.7(7)
O(8)	0.748(2)	0.1931(7)	0.3023(5)	7.4(7)
O(9)	0.895(2)	0.2020(8)	0.3905(7)	9(1)
O(10)	0.456(1)	0.2345(6)	0.7232(4)	4.9(6)
O(11)	0.764(3)	0.195(2)	0.773(1)	16(2)
N(1)	0.432(1)	0.0305(6)	0.7558(5)	2.5(5)
N(2)	0.512(1)	−0.0425(6)	0.6724(5)	3.1(6)
N(3)	0.474(1)	0.0881(6)	0.6395(4)	2.0(5)
N(4)	0.502(1)	0.1495(6)	0.6014(4)	2.1(5)
N(5)	0.614(1)	0.2032(7)	0.5173(5)	2.9(6)
N(6)	0.533(1)	0.3121(6)	0.5769(5)	2.8(5)
N(7)	0.194(1)	0.1764(7)	0.6375(5)	4.0(6)
N(8)	0.043(2)	0.1882(8)	0.6315(6)	4.8(7)
N(9)	−0.098(2)	0.199(1)	0.6279(8)	9(1)
N(10)	0.004(2)	0.034(1)	0.7092(7)	6(1)
N(11)	0.174(2)	0.3426(9)	0.5203(7)	4.4(8)
N(12)	0.761(2)	0.1942(8)	0.3603(7)	5.4(9)
C(1)	0.431(1)	0.0374(8)	0.8204(6)	2.8(7)
C(2)	0.490(2)	−0.025(1)	0.8586(6)	4.0(8)
C(3)	0.545(2)	−0.0946(9)	0.8358(6)	3.7(8)
C(4)	0.553(2)	−0.0996(9)	0.7739(7)	3.9(8)
C(5)	0.498(2)	−0.0369(8)	0.7360(6)	2.5(7)
C(6)	0.540(2)	0.0163(8)	0.6307(5)	2.5(7)
C(7)	0.634(1)	0.0002(8)	0.5803(6)	2.4(6)
C(8)	0.703(2)	−0.0748(8)	0.5712(6)	3.0(7)
C(9)	0.788(1)	−0.0871(8)	0.5211(7)	3.3(7)
C(10)	0.810(2)	−0.0267(9)	0.4811(6)	3.0(7)
C(11)	0.750(2)	0.0478(8)	0.4904(6)	2.9(7)
C(12)	0.659(1)	0.0619(8)	0.5403(6)	2.1(6)
C(13)	0.587(2)	0.1400(8)	0.5542(6)	2.5(7)
C(14)	0.618(2)	0.2844(8)	0.5325(6)	2.6(7)
C(15)	0.709(2)	0.334(1)	0.4966(6)	3.6(8)
C(16)	0.712(2)	0.4161(9)	0.5104(7)	3.8(8)
C(17)	0.633(2)	0.445(1)	0.5562(7)	4.0(8)
C(18)	0.549(2)	0.392(1)	0.5902(6)	3.0(7)
C(19)	0.369(2)	0.115(1)	0.8447(6)	4.5(8)
C(20)	0.467(2)	0.419(1)	0.6467(7)	6(1)
C(21)	0.812(4)	0.185(3)	0.838(2)	17(3)

[a] $B(\text{eq}) = (8\pi^2/3)\sum_{i=1}^{3}\sum_{j=1}^{3}U_{ij}\boldsymbol{a}_i^*\boldsymbol{a}_j^*\vec{a}_i\vec{a}_j$.

$[Cu_2(PPD35Me)(\mu_2\text{-}N_3)Br_3(CH_3OH)]$ (12). The diffraction intensities of a reddish-brown irregular platelike crystal of approximate dimensions 0.42 × 0.42 × 0.02 mm were collected using a Rigaku AFC6S diffractometer in a manner similar to that used for **1.** Hydrogen atoms were optimized by positional refinement with isotropic thermal parameters set 20% greater than those of their bonded partners. They were fixed for the final round of least-squares refinement. An absorption correction was performed using the analytical AGNOST method. A summary of crystal and other data is given in Table 1, and atomic coordinates are given in Table 6. Hydrogen atom coordinates (Table S17), anisotropic thermal parameters (Table S18), a full listing of bond distances and angles (Table 19), and least-squares planes data (Table S20) are included as supplementary material.

Table 5. Final Atomic Positional Parameters and B(eq) Values (Å^2) for $[Cu_2(PAN)(\mu_2\text{-}N_3)(\mu_2\text{-}NO_3)(NO_3)_2]\cdot CH_3OH\cdot CH_3CN$ (**5**)

atom	x	y	z	B(eq)[a]
Cu(1)	0.79448(8)	−0.00941(7)	0.1983(1)	4.00(8)
Cu(2)	0.82916(8)	0.12609(7)	0.2194(1)	3.98(8)
O(1)	0.8286(5)	−0.0598(4)	0.1013(6)	4.5(5)
O(2)	0.7118(5)	−0.0584(4)	0.0616(7)	6.7(6)
O(3)	0.7793(6)	−0.1148(4)	−0.0084(7)	7.4(6)
O(4)	0.9053(5)	0.1609(4)	0.1486(6)	5.4(5)
O(5)	0.8025(6)	0.1956(4)	0.0846(7)	6.5(6)
O(6)	0.9029(6)	0.2243(4)	0.0390(7)	8.1(7)
O(7)	0.9167	0.0751	0.3155	15.3
O(8)	0.9137	−0.0137	0.2823	27.2
O(9)	1.0041	0.0178	0.3837	25.6
O(10)	0.4651	0.1136	0.6742	5.3
O(11)	0.4571	0.1294	0.7169	9.2
N(1)	0.7817(7)	−0.0785(5)	0.2750(7)	4.5(6)
N(2)	0.6690(6)	−0.0450(5)	0.3085(7)	4.4(6)
N(3)	0.7332(5)	0.0372(4)	0.2757(6)	3.0(5)
N(4)	0.7429(5)	0.0965(4)	0.2783(6)	3.0(5)
N(5)	0.7121(5)	0.1900(4)	0.3184(6)	3.3(5)
N(6)	0.8381(6)	0.1917(4)	0.3070(6)	3.6(5)
N(7)	0.8105(5)	0.0614(5)	0.1336(6)	4.2(6)
N(8)	0.8299(7)	0.0612(5)	0.0569(9)	6.0(7)
N(9)	0.850(1)	0.0612(7)	−0.014(1)	11(1)
N(10)	0.7711(8)	−0.0783(5)	0.0495(8)	4.8(7)
N(11)	0.8702(8)	0.1952(6)	0.0893(9)	5.5(8)
N(12)	0.9462	0.0289	0.3170	17.8
N(13)	0.9095	0.2125	0.6357	9.6
C(1)	0.8341(8)	−0.1199(8)	0.283(1)	5.7(9)
C(2)	0.826(1)	−0.1717(7)	0.325(1)	7(1)
C(3)	0.763(1)	−0.1828(7)	0.361(1)	7(1)
C(4)	0.7080(9)	−0.1409(7)	0.352(1)	5.7(9)
C(5)	0.7213(9)	−0.0882(6)	0.3112(9)	4.1(8)
C(6)	0.6755(7)	0.0139(6)	0.3042(7)	3.1(6)
C(7)	0.6170(7)	0.0504(6)	0.3347(7)	3.2(7)
C(8)	0.5521(7)	0.0272(5)	0.3600(7)	3.7(7)
C(9)	0.4976(7)	0.0630(7)	0.3855(8)	3.7(7)
C(10)	0.4302(7)	0.0400(6)	0.4108(8)	4.5(8)
C(11)	0.3771(7)	0.0781(8)	0.431(1)	5.3(9)
C(12)	0.3877(7)	0.1372(7)	0.429(1)	5.4(9)
C(13)	0.4492(7)	0.1612(6)	0.4045(8)	4.7(7)
C(14)	0.5061(6)	0.1240(7)	0.3816(8)	3.7(7)
C(15)	0.5719(7)	0.1458(5)	0.3559(8)	3.8(7)
C(16)	0.6268(7)	0.1108(5)	0.3326(7)	2.9(6)
C(17)	0.6956(7)	0.1322(5)	0.3074(8)	3.2(7)
C(18)	0.7797(7)	0.2172(6)	0.3367(8)	3.3(7)
C(19)	0.7844(7)	0.2687(6)	0.3843(9)	4.1(7)
C(20)	0.851(1)	0.2964(6)	0.404(1)	5.7(9)
C(21)	0.9112(8)	0.2700(7)	0.378(1)	6(1)
C(22)	0.9031(7)	0.2177(7)	0.329(1)	5.3(9)
C(23)	0.9364	0.1809	0.5996	8.4
C(24)	0.9722	0.1348	0.5536	12.5
C(25)	0.5386	0.1003	0.6905	5.7
C(26)	1/2	0.1074	3/4	7.1

[a] $B(\text{eq}) = (8\pi^2/3)\sum^3_{i=1}\sum^3_{j=1}U_{ij}\boldsymbol{a}_i^*\boldsymbol{a}_j^*\vec{a}_i\cdot\vec{a}_j$.

Table 6. Final Atomic Positional Parameters and B(eq) Values (Å^2) for $[Cu_2(PPD35Me)(\mu_2\text{-}N_3)Br_3(CH_3OH)]$ (**12**)

atom	x	y	z	B(eq)[a]
Br(1)	0.26054(7)	0.06196(8)	0.7468(1)	5.03(8)
Br(2)	0.26491(6)	0.3026(1)	0.9142(1)	4.60(8)
Br(3)	0.47838(6)	0.2469(1)	0.6925(1)	5.34(8)
Cu(1)	0.27219(7)	0.2236(1)	0.7246(1)	3.75(9)
Cu(2)	0.39627(7)	0.3270(1)	0.6980(1)	3.64(8)
O(1)	0.3823(4)	0.3780(6)	0.8670(7)	5.5(6)
N(1)	0.1974(4)	0.2555(7)	0.6818(8)	3.5(6)
N(2)	0.1930(5)	0.3328(7)	0.6212(8)	3.3(6)
N(3)	0.2843(5)	0.3418(6)	0.6403(7)	3.3(6)
N(4)	0.3313(4)	0.3790(7)	0.6269(8)	3.0(6)
N(5)	0.3869(5)	0.4891(7)	0.5717(8)	3.6(6)
N(6)	0.4210(5)	0.4475(7)	0.6450(8)	3.9(6)
N(7)	0.3512(4)	0.2187(6)	0.7310(8)	3.6(6)
N(8)	0.3697(5)	0.1618(8)	0.791(1)	5.3(8)
N(9)	0.3856(6)	0.107(1)	0.843(1)	8(1)
C(1)	0.1482(6)	0.238(1)	0.712(1)	4.4(8)
C(2)	0.1116(7)	0.301(1)	0.669(1)	6(1)
C(3)	0.1427(7)	0.361(1)	0.613(1)	4.2(9)
C(4)	0.2406(6)	0.3748(8)	0.592(1)	3.4(7)
C(5)	0.2481(7)	0.447(1)	0.5167(9)	4.1(8)
C(6)	0.2978(7)	0.4850(9)	0.505(1)	4.4(9)
C(7)	0.3370(5)	0.4502(8)	0.565(1)	2.7(7)
C(8)	0.4115(7)	0.568(1)	0.532(1)	5(1)
C(9)	0.4579(6)	0.578(1)	0.579(1)	4.6(9)
C(10)	0.4614(6)	0.503(1)	0.649(1)	4.3(9)
C(11)	0.1366(6)	0.162(1)	0.784(1)	6(1)
C(12)	0.1254(6)	0.447(1)	0.558(1)	7(1)
C(13)	0.3828(6)	0.6276(9)	0.451(1)	6(1)
C(14)	0.5069(6)	0.4869(9)	0.729(1)	6(1)
C(15)	0.4184(8)	0.341(1)	0.946(1)	10(1)

[a] $B(\text{eq}) = (8\pi^2/3)\sum^3_{i=1}\sum^3_{j=1}U_{ij}\boldsymbol{a}_i^*\boldsymbol{a}_j^*\vec{a}_i\cdot\vec{a}_j$.

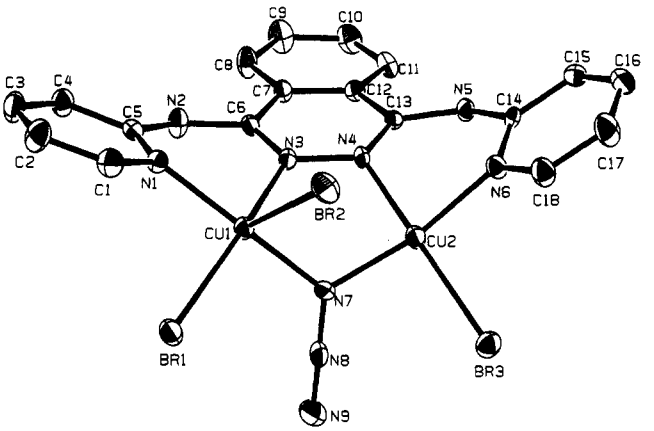

Figure 2. Structural representation of $[Cu_2(PAP)(\mu_2\text{-}N_3)Br_3]\cdot CH_2Cl_2$ (**1**) with hydrogen atoms omitted (50% probability thermal ellipsoids).

Results and Discussion

Description of the Structures of $[Cu_2(PAP)(\mu_2\text{-}N_3)Br_3]\cdot CH_2Cl_2$ (1), $[Cu_2(PAP6Me)(\mu_2\text{-}N_3)(\mu_2\text{-}Br)Br_2]\cdot 1.68H_2O$ (3), $[Cu_2(PAP6Me)(\mu_2\text{-}N_3)(\mu_2\text{-}H_2O)(NO_3)_2](NO_3)\cdot 0.75CH_3OH$ (4), $[Cu_2(PAN)(\mu_2\text{-}N_3)(\mu_2\text{-}NO_3)(NO_3)_2]\cdot CH_3OH\cdot CH_3CN$ (5), and $[Cu_2(PPD35Me)(\mu_2\text{-}N_3)Br_3(CH_3OH)]$ (12). The structure of **1** is shown in Figure 2, and bond distances and angles relevant to the copper coordination spheres are given in Table 7. Two essentially square-planar copper centers are bridged equatorially by the phthalazine and the μ_2-1,1-azide. A long contact to Br(2) (2.639(1) Å) might be considered to make Cu(1) square-pyramidal, but the longer Cu(2)−Br(2) distance (3.136(1) Å) does not generate a significant bridging interaction, and so Cu(2) is best described as square-planar. Terminal copper bromine distances are long (>2.4 Å), and copper−nitrogen distances are normal, with short (<1.97 Å) distances to the azide bridge. The Cu(1)−Cu(2) distance (3.169(1) Å) is quite long, in keeping with the fairly large azide bridge angle (108.7°). The asymmetry in the complex is shown also in the Cu−N−N (diazine) angles, which differ (Cu(1)−N(3)−N(4) 114.4°, Cu(2)−N(4)−N(3) 116.9°) but are normal for this sort of complex. The azide is linear, and the sum of the angles around N(7) (359.5°) indicates no pyramidal distortion at the azide bridge. The ligand is slightly twisted, with dihedral angles of 23.1 and 33.6° between the phthalazine mean plane and the mean planes of the pyridine rings defined by N(1) and N(6), respectively.

The structure of **3** is shown in Figure 3, and bond distances and angles relevant to the copper coordination spheres are given in Table 8. The two distorted square-pyramidal copper centers are bridged equatorially by the phthalazine and a μ_2-1,1-azide and weakly by an axial bromine. Other terminal ligands include pyridine and bromine. The bridging copper−bromine distance (Cu(1)−Br(1)) is quite long (2.755(3)Å), while the terminal

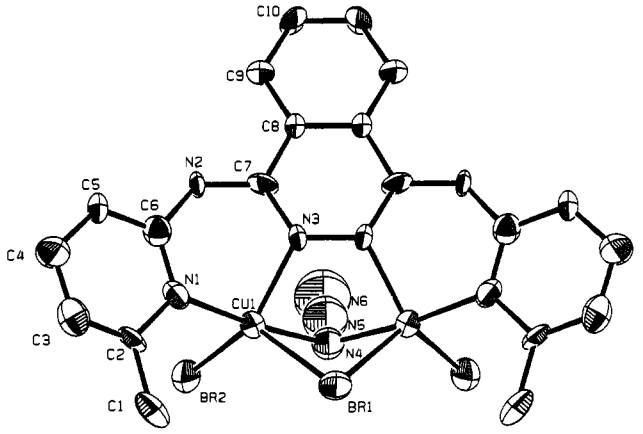

Figure 3. Structural representation of $[Cu_2(PAP6Me)(\mu_2\text{-}N_3)(\mu_2\text{-}Br)Br_2]\cdot 1.68H_2O$ (**3**) with hydrogen atoms omitted (50% probability thermal ellipsoids).

Table 7. Interatomic Distances (Å) and Angles (deg) Relevant to the Copper Coordination Spheres in $[Cu_2(PAP)(\mu_2\text{-}N_3)Br_3]\cdot CH_2Cl_2$ (**1**)

Br(1)–Cu(1)	2.432(1)	Cu(2)–N(4)	2.031(5)
Br(2)–Cu(1)	2.639(1)	Cu(2)–N(6)	1.974(5)
Br(3)–Cu(2)	2.410(1)	Cu(2)–N(7)	1.936(5)
Cu(1)–N(1)	1.994(5)	N(7)–N(8)	1.213(7)
Cu(1)–N(3)	2.034(5)	N(8)–N(9)	1.131(7)
Cu(1)–N(7)	1.965(5)	Cu(1)–Cu(2)	3.169(1)
Br(1)–Cu(1)–Br(2)	101.90(4)	Br(3)–Cu(2)–N(6)	95.7(1)
Br(1)–Cu(1)–N(1)	92.1(1)	Br(3)–Cu(2)–N(7)	94.0(2)
Br(1)–Cu(1)–N(3)	159.7(2)	N(4)–Cu(2)–N(6)	86.3(2)
Br(1)–Cu(1)–N(7)	93.1(1)	N(4)–Cu(2)–N(7)	85.6(2)
Br(2)–Cu(1)–N(1)	103.0(1)	N(6)–Cu(2)–N(7)	168.8(2)
Br(2)–Cu(1)–N(3)	98.0(1)	Cu(1)–N(3)–N(4)	114.4(3)
Br(2)–Cu(1)–N(7)	88.7(2)	Cu(2)–N(4)–N(3)	116.9(3)
N(1)–Cu(1)–N(3)	87.2(2)	Cu(1)–N(7)–Cu(2)	108.7(3)
N(1)–Cu(1)–N(7)	165.9(2)	Cu(1)–N(7)–N(8)	124.7(4)
N(3)–Cu(1)–N(7)	83.4(2)	Cu(2)–N(7)–N(8)	126.1(4)
Br(3)–Cu(2)–N(4)	165.7(2)	N(7)–N(8)–N(9)	179.6(7)

Table 8. Interatomic Distances (Å) and Angles (deg) Relevant to the Copper Coordination Spheres in $[Cu_2(PAP6Me)(\mu_2\text{-}N_3)(\mu_2\text{-}Br)Br_2]\cdot 1.68H_2O$ (**3**)

Br(1)–Cu(1)	2.755(3)	1[a]	Cu(1)–N(1)	1.992(9)	1[a]
Br(1)–Cu(1)	2.755(3)	4[a]	Cu(1)–N(3)	2.048(9)	1[a]
Br(2)–Cu(1)	2.433(2)	1[a]	Cu(1)–N(4)	1.944(9)	1[a]
Cu(1)–Cu(1′)	3.203(3)				
Cu(1)–Br(1)–Cu(1)	71.11(9)		Cu(1)–N(4)–N(5)	112.7(8)	
Br(1)–Cu(1)–Br(2)	126.86(9)		N(4)–N(5)–N(6)	177(3)	
Br(1)–Cu(1)–N(1)	102.9(3)		N(1)–Cu(1)–N(3)	88.4(4)	
Br(1)–Cu(1)–N(3)	89.0(3)		N(1)–Cu(1)–N(4)	173.8(5)	
Br(1)–Cu(1)–N(4)	77.7(5)		N(3)–Cu(1)–N(4)	85.5(5)	
Br(2)–Cu(1)–N(1)	94.7(3)		Cu(1)–N(1)–C(2)	122.3(8)	
Br(2)–Cu(1)–N(3)	141.8(3)		Cu(1)–N(1)–C(6)	121.1(8)	
Br(2)–Cu(1)–N(4)	89.8(4)		Cu(1)–N(3)–N(3)	116.7(2)	
Cu(1)–N(4)–Cu(1)	110.9(8)				

[a] ADC(*).

copper–bromine distance is much shorter (2.433(2) Å). Copper–nitrogen distances are normal (<2.05 Å), with a tightly bound bridging azide. The Cu–Cu separation (3.203(3)Å) is consistent with other PAP6Me complexes involving hydroxide bridges, and the expanded dinuclear center is seen as a result of a steric effect associated with the methyl group on the pyridine 6-position.[6] The azide bridge angle is quite large (110.9(8)°), but again consistent with the Cu–OH–Cu angle in the analogous complex $[Cu_2(PAP6Me)(\mu_2\text{-}OH)(\mu_2\text{-}Cl)Cl_2]\cdot 3H_2O$ (111.6°).[18] The molecule is bisected by a plane of symmetry passing through the phthalazine and the bridging azide, and the Cu–N–N (diazine) angles are equal (116.7°) and slightly larger than those found in **1**. The azide group could not be modeled anisotropically, which could be the result of the presence of two conformations which are very close together, but both in the symmetry plane. The sum of the angles at N(4) is nominally 336.3°, which under normal circumstances would represent a significant pyramidal distortion at the bridging nitrogen. However, in view of the disorder at N(4), which lies in the mirror plane, actually quantifying the distortion may be difficult. The ligand is twisted about the phthalazine subunit, with an angle of 28.9° between the phthalazine and pyridine mean planes. A diffuse, partially occupied water molecule, with less than unit occupancy, occurs in the asymmetric unit.

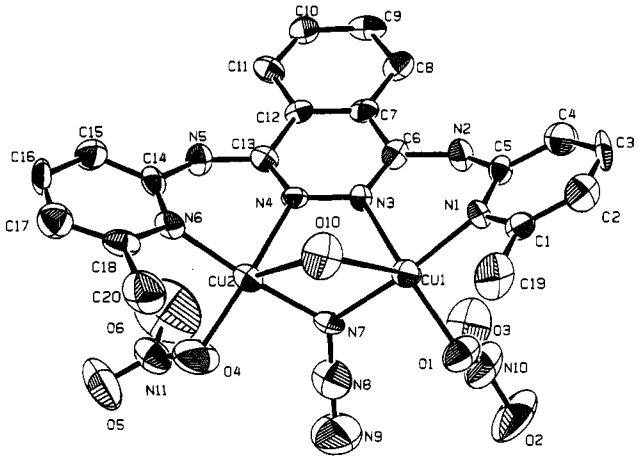

Figure 4. Structural representation of $[Cu_2(PAP6Me)(\mu_2\text{-}N_3)(\mu_2\text{-}H_2O)(NO_3)_2](NO_3)\cdot 0.75CH_3OH$ (**4**) with hydrogen atoms omitted (50% probability thermal ellipsoids).

Table 9. Interatomic Distances (Å) and Angles (deg) Relevant to the Copper Coordination Spheres in $[Cu_2(PAP6Me)(\mu_2\text{-}N_3)(\mu_2\text{-}H_2O)(NO_3)_2](NO_3)\cdot 0.75CH_3OH$ (**4**)

Cu(1)–O(1)	1.985(9)	Cu(2)–O(4)	1.94(1)
Cu(1)–N(1)	1.95(1)	Cu(2)–N(4)	2.00(1)
Cu(1)–N(3)	1.992(9)	Cu(2)–N(6)	1.96(1)
Cu(1)–N(7)	1.96(1)	Cu(2)–N(7)	1.93(1)
Cu(1)–O(10)	2.55(1)	Cu(2)–O(10)	2.659(9)
Cu(1)–Cu(2)	3.217(3)		
O(1)–Cu(1)–N(1)	93.8(4)	Cu(1)–N(3)–N(4)	118.3(8)
O(1)–Cu(1)–N(3)	159.9(4)	Cu(2)–N(4)–N(3)	117.2(7)
O(1)–Cu(1)–N(7)	91.8(4)	Cu(1)–N(7)–Cu(2)	111.7(5)
N(1)–Cu(1)–N(3)	89.0(4)	Cu(1)–N(7)–N(8)	123(1)
N(1)–Cu(1)–N(7)	174.4(4)	Cu(2)–N(7)–N(8)	124(1)
N(3)–Cu(1)–N(7)	85.6(4)	N(4)–Cu(2)–N(6)	89.8(4)
O(4)–Cu(2)–N(4)	157.8(5)	N(4)–Cu(2)–N(7)	87.0(4)
O(4)–Cu(2)–N(6)	91.9(5)	N(6)–Cu(2)–N(7)	173.8(5)
O(4)–Cu(2)–N(7)	93.0(5)		

The structure of the dinuclear complex **4** is illustrated in Figure 4, and bond distances and angles relevant to the copper coordination spheres are give in Table 9. The two square-pyramidal copper centers are bridged by the diazine and a μ_2-1,1-azide, but in addition, a water molecule also acts as a weak axial bridge, with relatively long bond distances (Cu(1)–O(10) 2.55(1) Å, Cu(2)–O(10) 2.659(9) Å). This is a most unusual situation for water. Two monodentate nitrates complete the basal coordination sites. Cu(1) and Cu(2) are displaced by 0.179 and 0.137 Å from their respective basal ligand mean planes, which are mutually inclined by 39.6°. The Cu–Cu separation (3.217(3) Å) and the azide bridge angle (111.7(5)°) are again consistent with comparable hydroxide-bridged complexes.[6] In-plane copper–ligand distances are quite short (2.0 Å or less), and the sum of the angles around N(7) (358.7°) indicates an essentially trigonal planar azide bridge. The ligand adopts a

(18) Mandal, S. K.; Woon, T. C.; Thompson, L. K.; Newlands, M. J.; Gabe, E. J. *Aust. J. Chem.* **1986**, *39*, 1007.

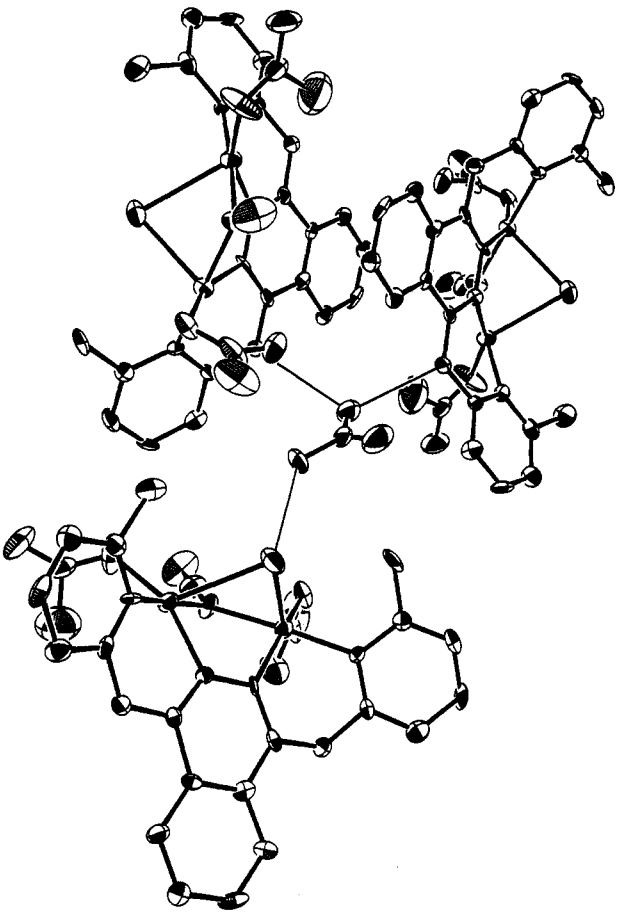

Figure 5. Extended structural representation for **4** showing the hydrogen-bonding scheme involving ionic nitrate N(12)−O(7)−O(8)−O(9).

twisted conformation with angles of 29.8 and 23.5° between pyridine mean planes defined by N(1) and N(6) and the phthalazine mean plane, respectively, and an angle of 46.8° between the pyridine rings themselves.

While the dinuclear complex itself is essentially normal, the lattice arrangement of these complex units warrants further discussion. The ionic nitrate creates an unusual, extended hydrogen-bonding network, part of which is illustrated in Figure 5, in which O(7) is weakly hydrogen bonded to hydrogen atoms on exocyclic nitrogen atoms N(2) and N(5) on two adjacent molecules (O(7)−N(5) 2.87 Å; O(7)−N(2) 2.89 Å) and O(8) is weakly hydrogen bonded to the bridging water (O(10)) on a third. An intriguing consequence of this arrangement is the proximity of the fused benzene rings of the phthalazine groups in adjacent molecules, which are essentially coplanar but are forced together as a result of the hydrogen-bonding network with a very short benzene−benzene ring separation (3.2 Å), which is less than that in graphite.

The structural representation for **5** is given in Figure 6, and bond distances and angles relevant to the copper coordination spheres are given in Table 10. Two square-pyramidal copper centers are bridged equatorially by the tetradentate naphthalazine−diazine ligand and the μ_2-1,1-azide and axially by a rather loosely bound bidentate bridging nitrate. The large thermal parameters associated with this group, in particular for O(8) and O(9), are an indication of the difficulty of "fixing" this group in the structural analysis and may be associated with the crystal instability in the X-ray beam. However the otherwise normal structural features of the dinuclear center indicate that the bridging nitrate is real. Two monodentate nitrates complete the basal donor set. The Cu−Cu separation (3.188(2) Å) and the

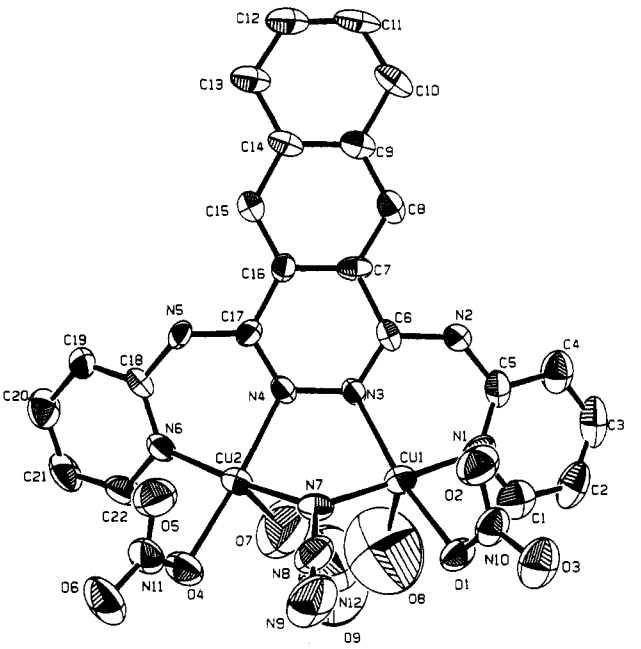

Figure 6. Structural representation of $[Cu_2(PAN)(\mu_2\text{-}N_3)(\mu_2\text{-}NO_3)(NO_3)_2].CH_3OH{\cdot}CH_3CN$ (**5**) with hydrogen atoms omitted (50% probability thermal ellipsoids).

Table 10. Interatomic Distances (Å) and Angles (deg) Relevant to the Copper Coordination Spheres in $[Cu_2(PAN)(\mu_2\text{-}N_3)(\mu_2\text{-}NO_3)(NO_3)_2]{\cdot}CH_3OH{\cdot}CH_3CN$ (**5**)

Cu(1)−O(1)	1.991(8)	Cu(1)−N(1)	1.97(1)
Cu(1)−N(3)	2.006(9)	Cu(1)−N(7)	1.92(1)
Cu(1)−O(8)	2.327(2)	Cu(2)−O(7)	2.311(2)
Cu(2)−O(4)	2.011(9)	Cu(2)−N(4)	2.020(9)
Cu(2)−N(6)	1.97(1)	Cu(2)−N(7)	1.94(1)
Cu(1)−Cu(2)	3.188(2)		
O(1)−Cu(1)−N(1)	90.2(4)	O(1)−Cu(1)−N(3)	164.2(4)
O(1)−Cu(1)−N(7)	93.7(4)	Cu(1)−N(7)−Cu(2)	111.1(4)
N(1)−Cu(1)−N(3)	89.7(5)	Cu(1)−N(7)−N(8)	122(1)
N(1)−Cu(1)−N(7)	174.9(4)	Cu(2)−N(7)−N(8)	123(1)
N(3)−Cu(1)−N(7)	87.5(4)	N(7)−N(8)−N(9)	178(2)
O(4)−Cu(2)−N(4)	172.4(4)	O(4)−Cu(2)−N(6)	91.2(4)
O(4)−Cu(2)−N(7)	93.0(4)	N(4)−Cu(2)−N(6)	89.3(4)
N(4)−Cu(2)−N(7)	86.1(4)	N(6)−Cu(2)−N(7)	174.6(5)
Cu(1)−N(3)−N(4)	117.7(8)	Cu(2)−N(4)−N(3)	115.4(8)

azide bridge angle (111.1(4)°) are quite large but consistent with systems of this sort with bidentate, axial bridging ligands, which have the effect of forcing the metal centers apart.[6] The sum of the angles at N(7) is 356.1°, indicating little pyramidal distortion at the azide bridge. Cu(1) and Cu(2) are displaced by 0.131 and 0.095 Å, respectively, from their mean basal ligand planes toward the axial ligating group. The complex is bent about the diazine group, as usual, with angles of 24.4 and 31.9°, respectively, between the N(1) and N(6) pyridine mean planes and the naphthalazine mean planes. The unique feature of this complex is, of course, the ligand itself, where the diazine group has been extended by the addition of a fused benzene ring, compared with the phthalazines. As expected the naphthalazine unit is itself essentially planar, and in most respects PAN compares closely with its phthalazine counterparts. A detailed description of the coordination chemistry of this ligand, and other related ligands, will be presented elsewhere.[19]

The structural representation of **12** is given in Figure 7, and bond distances and angles relevant to the copper coordination spheres are given in Table 11. The ligand PPD35Me belongs to the 5,6,5 class (**I**) and creates a much larger dinuclear center

(19) Manuel, M. E.; Thompson, L. K.; Tandon, S. S. Unpublished results.

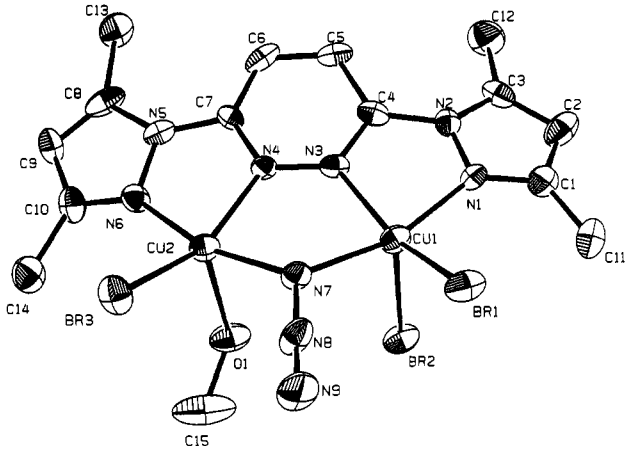

Figure 7. Structural representation of $[Cu_2(PPD35Me)(\mu_2\text{-}N_3)Br_3(CH_3OH)]$ (**12**) with hydrogen atoms omitted (50% probability thermal ellipsoids).

Table 11. Interatomic Distances (Å) and Angles (deg) Relevant to the Copper Coordination Spheres in $[Cu_2(PPD35Me)(\mu_2\text{-}N_3)Br_3(CH_3OH)]$ (**12**)

Br(1)−Cu(1)	2.372(2)	Cu(1)−N(7)	2.00(1)
Br(2)−Cu(1)	2.691(2)	Cu(2)−N(4)	2.02(1)
Br(3)−Cu(2)	2.376(2)	Cu(2)−N(6)	1.97(1)
Cu(1)−N(1)	2.02(1)	Cu(2)−N(7)	1.98(1)
Cu(1)−N(3)	2.04(1)	Cu(2)−O(1)	2.313(8)
Cu(1)−Cu(2)	3.487(2)		
Br(1)−Cu(1)−Br(2)	107.55(7)	Cu(1)−N(7)−Cu(2)	122.5(5)
Br(1)−Cu(1)−N(1)	98.1(3)	Cu(1)−N(7)−N(8)	115.6(9)
Br(1)−Cu(1)−N(3)	154.9(3)	Cu(2)−N(7)−N(8)	116.5(9)
Br(1)−Cu(1)−N(7)	94.8(3)	N(7)−N(8)−N(9)	177(2)
Br(2)−Cu(1)−N(1)	94.8(3)	Cu(2)−N(4)−N(3)	121.4(8)
Br(2)−Cu(1)−N(3)	97.6(3)	Cu(1)−N(3)−N(4)	123.3(9)
Br(2)−Cu(1)−N(7)	92.7(3)	N(6)−Cu(2)−N(7)	162.5(5)
N(1)−Cu(1)−N(3)	78.8(5)	N(4)−Cu(2)−N(7)	85.6(4)
N(1)−Cu(1)−N(7)	162.3(4)	N(4)−Cu(2)−N(6)	76.9(5)
N(3)−Cu(1)−N(7)	84.3(5)	Br(3)−Cu(2)−N(6)	98.3(3)
Br(3)−Cu(2)−N(4)	151.2(3)	Br(3)−Cu(2)−N(7)	97.0(3)

than those found in **1** and **3**−**5**. The Cu−Cu separation (3.487(2) Å) and azide bridge angle (Cu(1)−N(7)−Cu(2) = 122.5(5)°) are very large and consistent with previous examples involving the ligands PPD and PPD3Me (Figure 1).[5] The two square-pyramidal copper centers are bridged by just the diazine and the μ_2-1,1-azide, with two bromines completing the coordination sphere of Cu(1) and a bromine and a fairly tightly bound axial methanol at Cu(2) (Cu(2)−O(1) 2.313(8) Å). The overall molecule is essentially flat with angles of 18.2 and 15.5° between the pyrazole least-squares planes defined by N(2) and N(5), respectively, and the pyridazine plane and an angle of 32.2° between the mean pyrazole planes. The copper centers are displaced by 0.362 Å (Cu(1)) and 0.371 Å (Cu(2)) from their respective basal ligand mean planes. The sum of the angles at the azide bridge (354.6°) indicates a very slight pyramidal distortion at the bridging atom N(7).

Spectroscopic Properties. Infrared absorptions associated with the azide bridge (Table 12) reveal a pattern that is essentially similar to that observed previously,[5] with one main absorption at >2060 cm^{-1}, which is associated with the μ_2-1,1-azide bridge. Additional absorptions for **1**, **4** and for **6**, **7**, which appear as shoulders or secondary bands, may be associated with disorder or asymmetry in the structures. The band at 2044 cm^{-1} for **4** is unusual in the light of the structure. The presence of ν_{as} azide bands for **8**−**10** in two ranges (>2060 cm^{-1} and <2060 cm^{-1}) suggests an azide bridge and two terminal azides in each case, consistent with the structure of **12**. The nitrate, perchlorate, and triflate groups appear to be uncoordinated. These three compounds also have very similar electronic absorption spectra (Table 12), consistent with four-coordinate copper(II) centers. The long-wavelength visible absorption for **12** is consistent with five-coordinate copper ions involving bromine coordination, and the higher energy band for **11** would be consistent with a similar structure involving bonded chlorine. Compounds **6** and **7** have electronic spectra similar to those of **11** and **12**, and it is reasonable to assume a similar structural arrangement.

Magnetic Susceptibility Studies. Room-temperature magnetic moments (μ_{eff}) for **1**−**5** (Table 12) fall in the range 1.33−1.65 μ_B (300 K), indicative of the presence of weak to moderate antiferromagnetic intradimer interactions. In sharp contrast, compounds **6**−**12** have much lower room-temperature moments (<0.6 μ_B) indicative of very strong antiferromagnetic coupling. Variable-temperature magnetic studies (4−300 K) were carried out on powdered samples of all of the complexes. The theoretical expression for the magnetic susceptibility of a copper(II) dimer is given by eq 1,[20] where N, β, and k have their usual

$$\chi_m = \frac{N\beta^2 g^2}{3k(T-\Theta)}[1 + {}^1/_3 \exp(-2J/kT)]^{-1}(1-\varrho) + \frac{(N\beta^2 g^2)\varrho}{4kT} + N\alpha \quad (1)$$

meaning, $N\alpha$ is the temperature-independent paramagnetism, ϱ represents the fraction of a possible magnetically dilute impurity, and χ_m is expressed per mole of copper metal. Θ is a Weiss-like correction to account for possible intermolecular exchange effects or zero-field splitting. The variable-temperature magnetic susceptibility profiles for **6**−**12** are typical for strongly antiferromagnetically coupled systems, with a slight rise in χ_m at high temperatures to a maximum well above room-temperature. The data for these compounds were fitted to eq 1 using a nonlinear regression procedure with g, J, ϱ, and Θ as variables. In all cases, good data fits were obtained with $-2J$ values in the range 768−932 cm^{-1} (Table 13), indicating the presence of very strong net antiferromagnetic coupling. The experimental data and the best fit line for **12** (solid line) are shown in Figure 8 for g = 2.21(2), $2J$ = −921(9) cm^{-1}, ϱ = 0.0041, $N\alpha = 61 \times 10^{-6}$ emu, and Θ = 1 K. The agreement factor (10^2R) is small, indicating a good data fit. The sharp rise in susceptibility at low temperatures is associated with a small amount of paramagnetic impurity. Very large azide bridge angles are anticipated for **6**−**11**, comparable with that of **12** (122.5°), on the basis of the "bite" of these 5,6,5 ligands and the structures of related compounds already reported.[5] As has been discussed previously,[5] at large azide bridge angles, the dominant magnetically active exchange bridge of the two that link the two copper centers in a parallel fashion is the azide. The pyridazine bridge has been shown to propagate moderately strong antiferromagnetic coupling in a planar dinuclear copper(II) complex involving just two pyridazine bridges ($-2J$ = 536 cm^{-1}),[21] with Cu−N−N (diazine) angles of 126.8 and 127.3°. The smaller Cu−N−N (diazine) bridge angles in **12** (121.4 and 123.2°), and likely those in **6**−**11** also, would reasonably suggest somewhat weaker coupling due to the diazine bridges in **6**−**12**.

The situation for **1**−**5** is, however, quite different. Collectively they are much more weakly antiferromagnetically coupled than **6**−**12**. However, fitting of the magnetic data to eq 1 was much more difficult and required the use of significant negative Θ values. For **2**, **3**, and **5**, Θ corrections were limited

(20) Bleaney, B.; Bowers, K. D. *Proc. R. Soc. London* **1952**, *A214*, 451.
(21) Abraham, F.; Lagrenee, M.; Sueur, S.; Mernari, B.; Bremard, C. *J. Chem. Soc., Dalton Trans.* **1991**, 1443.

Table 12. Spectroscopic and Magnetic Properties

complex	μ_{eff}(RT) (μ_B)	electronic data (nm)[a]	infrared data (cm^{-1}): ν_{as} (N_3^-)
$[Cu_2(PAP)(\mu_2\text{-}N_3)Br_3]\cdot CH_2Cl_2$ (**1**)	1.33	[450], 510, [660], 730	[2095, [2052]
$[Cu_2(PAP6Me)(N_3)Cl_3]\cdot CH_2Cl_2$ (**2**)	1.65	380, 430, [500], 720,900	2072
$[Cu_2(PAP6Me)(\mu_2\text{-}N_3)(\mu_2\text{-}Br)Br_2]\cdot 0.5CH_3OH$ (**3**)	1.47	385, [440], 550, 730	2068
$[Cu_2(PAP6Me)(\mu_2\text{-}N_3)(\mu_2\text{-}H_2O)(NO_3)_2](NO_3)$ (**4**)	1.46	380, [440], 630	2094, 2044
$[Cu_2(PAN)(\mu_2\text{-}N_3)(\mu_2\text{-}NO_3)(NO_3)_2]\cdot CH_3OH\cdot CH_3CN\cdot 4.5H_2O$ (**5**)	1.55	370, 390, 410, 610	2100
$[Cu_2(PPD)(\mu_2\text{-}N_3)Cl_3]\cdot 0.5CH_3OH\cdot 1.5H_2O$ (**6**)	0.48	390, 445, 675	2090, 2083
$[Cu_2(PPD)(\mu_2\text{-}N_3)Br_3]\cdot 0.5H_2O$ (**7**)	0.39	[410], 475, 690	2084, [2036]
$[Cu_2(PPD)(\mu_2\text{-}N_3)(N_3)_2](NO_3)\cdot 0.5H_2O$ (**8**)	0.45	[400], [470], 675	2087, 2043 1768,1745[b]
$[Cu_2(PPD)(\mu_2\text{-}N_3)(N_3)_2](ClO_4)$ (**9**)	0.43	415, [490], 645	2082, 2037 1109[c]
$[Cu_2(PPD)(\mu_2\text{-}N_3)(N_3)_2]$ $(CF_3SO_3)\cdot 0.5CH_3OH$ (**10**)	0.57	[400], 475, 680	2082, 2066, 2040
$[Cu_2(PPD35Me)(\mu_2\text{-}N_3)Cl_3]\cdot CH_3OH$ (**11**)	0.51	475, 720	2082
$[Cu_2(PPD35Me)(\mu_2\text{-}N_3)Br_3(CH_3OH)]$ (**12**)	0.45	365, 445, [505], 800	2077

[a] Mull transmittance. [b] $\nu_1+\nu_4(NO_3^-)$. [c] $\nu_3(ClO_4^-)$.

Table 13. Variable-Temperature Magnetic Properties[a]

complex	g	$-2J$ (cm^{-1})	ϱ	Θ (K)	TIP $\times 10^6$ (emu)	10^2R[b]
$[Cu_2(PAP)(\mu_2\text{-}N_3)Br_3]\cdot CH_2Cl_2$ (**1**)	2.08(9)	241(10)	0.003	−80	76	2.6
$[Cu_2(PAP6Me)(N_3)Cl_3]\cdot CH_2Cl_2$ (**2**)	2.01(6)	112(4)	0.01	−4	68	4.2
	2.27(6)	88(4)	0.012	−64	52	1.0
$[Cu_2(PAP6Me)(\mu_2\text{-}N_3)(\mu_2\text{-}Br)Br_2]\cdot 1.68H_2O$ (**3**)	2.01(8)	234(10)	0.014	−5	80	4.3
	2.20(9)	231(10)	0.016	−50	75	2.9
$[Cu_2(PAP6Me)(\mu_2\text{-}N_3)(\mu_2\text{-}H_2O)(NO_3)_2](NO_3)$ (**4**)	2.01(4)	187(7)	0.08	0	76	9.2
	2.11(3)	111(6)	0.06	−115	68	3.8
$[Cu_2(PAN)(\mu_2\text{-}N_3)(\mu_2\text{-}NO_3)(NO_3)_2]\cdot CH_3OH\cdot CH_3CN\cdot 4.5H_2O$ (**5**)	2.04(2)	220(5)	0.029	−6	100	4.1
	2.18(2)	187(4)	0.028	−76	100	3.3
$[Cu_2(PPD)(\mu_2\text{-}N_3)Cl_3]\cdot 0.5CH_3OH\cdot 1.5H_2O$ (**6**	2.17(3)	870(11)	0.003	−2	60	2.2
$[Cu_2(PPD)(\mu_2\text{-}N_3)Br_3]\cdot 0.5H_2O$ (**7**)	2.23(9)	932(16)	0.0007	−2	47	2.0
$[Cu_2(PPD)(\mu_2\text{-}N_3)(N_3)_2](NO_3)\cdot 0.5H_2O$ (**8**)	2.14(4)	906(20)	0.0058	−1	56	3.8
$[Cu_2(PPD)(\mu_2\text{-}N_3)(N_3)_2](ClO_4)$ (**9**)	2.13(6)	829(11)	0.00031	0	32	1.9
$[Cu_2(PPD)(\mu_2\text{-}N_3)(N_3)_2]$ $(CF_3SO_3)\cdot 0.5CH_3OH$ (**10**)	2.08(6)	768(24)	0.0058	−1	87	4.7
$[Cu_2(PPD35Me)(\mu_2\text{-}N_3)Cl_3]\cdot CH_3OH$ (**11**)	2.26(1)	846(5)	0.009	−1	40	2.3
$[Cu_2(PPDMe2)(\mu_2\text{-}N_3)Br_3(CH_3OH)]$ (**12**)	2.21(2)	921(9)	0.0041	1	61	1.6

[a] Magnetic measurements were done, where possible, on the same, uniform sample from which crytals were chosen for X-ray analysis. [b] $R = [\Sigma(\chi_{obs} - \chi_{calc})^2/\Sigma\chi_{obs}2]^{1/2}$.

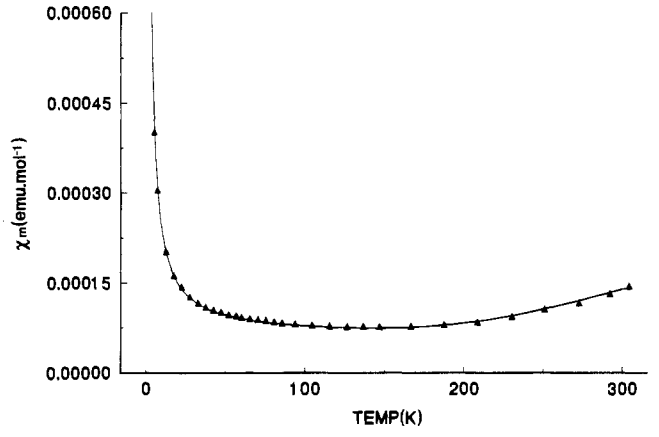

Figure 8. Magnetic data for $[Cu_2(PPD35Me)(\mu_2\text{-}N_3)Br_3(CH_3OH)]$ (**12**). The solid line was calculated from eq 1 with $g = 2.21(2)$, $2J = -921(9)$ cm^{-1}, $\varrho = 0.0041$, $N\alpha = 61 \times 10^{-6}$ emu, and $\Theta = 1$ K ($10^2R = 1.6$).

in an initial analysis to small values, and for $-\Theta$ in the range 4−6 K fitting parameters (10^2R) (4.1−4.3) were found to be substantially higher than would normally be considered acceptable. $-2J$ values for these compounds fall in the range 112−234 cm^{-1} (consistent with $T(\chi_{max})$), a dramatic reduction when compared with those for **6**−**12**, but consistent with the much smaller azide bridge angles which result from the restricted bite of the 6,6,6 diazine ligands (**I**).[5] For **4** the data fit was much worse, but $-2J$ fell in the same range. For **3**−**5** the azide bridge angles are in the range 110.9−111.7°, where the azide is expected to propagate antiferromagnetic exchange in its μ_2-1,1-mode.[5] The magnetic data for **1** did not fit eq 1 sensibly with small Θ values, and gave g values of <1.85. In this case it is noteworthy that the Cu−N_3−Cu bridge angle is 108.7(3)°, very close to the critical angle range at which the azide bridge changes from ferromagnetic to antiferromagnetic behavior.[5]

Small Θ corrections are often included in such data analyses, and negative values are indicative of the presence of antiferromagnetic intermolecular exchange effects. However the corrections are usually small and may result from weak lattice associations or hydrogen-bonding interactions. The structures of **1** and **3**−**5** do not show any intermolecular associations that would suggest significant intermolecular magnetic exchange effects, even for compound **4**, which displays extensive hydrogen-bonded associations (Figure 5). Given the rather poor data fits for **1**−**5** in general, regression analyses of eq 1 were carried out with much larger Θ ranges. Improved data fits were obtained for **2**−**5** (see Table 13), and for **1** with $\Theta = -80$ K a reasonable data fit was obtained with a sensible g value. The apparent necessity for large negative Θ values in most of these data analyses raises the question of the appropriateness of the Bleaney−Bowers equation to solve magnetic problems associated with dinuclear copper(II) complexes of this type with weak to moderate antiferromagnetic coupling and two dissimilar, parallel magnetic bridges. Clearly for **6**−**12**, which are much more strongly coupled, this does not constitute a problem.

Studies by Kahn et al.[22,23] have attempted to deal with the

(22) Mallah, T.; Boillot, M.-L.; Kahn, O.; Gouteron, J.; Jeannin, S.; Jeannin, Y. *Inorg. Chem.* **1986**, *25*, 3058.
(23) Kahn, O.; Mallah, T.; Gouteron, J.; Jeannin, S.; Jeannin, Y. *J. Chem. Soc., Dalton Trans.* **1989**, 1117.

problem of differentiating the exchange contributions in an asymmetric, dibridged, dinuclear copper(II) complex (Cu[X,Y]-Cu). Combinations of phenoxide with e.g. hydroxide, alkoxide, azide, and cyanate were investigated by assuming the "active electron approximation". The two different bridges can be considered to act in a complementary or anticomplementary fashion.[24-26] The complementary case involves overlap integrals (S_X,S_Y) of the same sign, while the anticomplementary case involves overlap integrals of opposite sign. Typically combinations of phenoxide with azide have net exchange integrals which reflect two bridge contributions of different sign ($J_T = J_F + J_{AF}$) and are antiferromagnetic overall, but with $|J|$ values which are substantially lower than those observed for phenoxide/hydroxide or phenoxide/alkoxide combinations with comparable phenoxide bridge angles.[27-31] This effect is attributed to the fact that the μ_2-1,1-azide bridge behaves ferromagnetically.

In all these complexes the largest Cu−N_3−Cu bridge angle is 106.1°, which is below the experimentally observed value for the change in magnetic behavior from ferromagnetic to antiferromagnetic for dinuclear copper(II) complexes with parallel combinations of azide and diazine bridges.[5] Therefore the reduced antiferromagnetic behavior in all these complexes is reasonable, and their magnetic data have been analyzed successfully using the Bleaney−Bowers equation. It is also apparent, and reasonable, that when the ferromagnetic bridge dominates e.g. in $[Cu_2(Famp)(OCN)](ClO_4)_2$, involving a combination of cyanate-*O* and phenoxide bridges ($2J = 43$ cm^{-1}),[31] and in some copper(II) azide/diazine complexes,[5] that the Bleaney−Bowers equation is also obeyed.[2,32] However, despite the hint apparent in earlier papers,[22,23] the "resultant" effect of two different, parallel, magnetically active bridges, both of which stabilize the "same" ground state (i.e antiferromagnetic/antiferromagnetic or ferromagnetic/ferromagnetic combinations), has not been conclusively researched or established. However, in most instances involving a phenoxide bridge in combination with hydroxide or alkoxide, where both bridges have comparable and quite large antiferromagnetic exchange effects (e.g. $-2J_{net} > 380$ cm^{-1}),[22,23] reasonable fits of the variable-temperature magnetic data to the Bleaney−Bowers equation have been reported. Also for the strongly coupled complexes **6**−**12** acceptable data fits to eq 1 were obtained.

The Bleaney−Bowers equation involves a single exchange integral for a dicopper(II) complex and does not take into account the number and nature of the groups that act as superexchange bridges. It defines a single singlet−triplet energy scheme, whose ground term will vary depending on the overall nature of the exchange interaction (i.e. ferromagnetic or antiferromagnetic). If the dinuclear complex has a single bridge or a symmetrical double bridge (e.g. as in the case of the symmetrical dihydroxy-bridged complexes[1] or symmetrical dipyridazine- or diphthalazine-bridged dicopper(II) complexes,[21,33,34] the system can be successfully described using one exchange integral, and technically this defines the exchange integral for that particular bridge. Asymmetric dibridged systems of the type under consideration have, so far, all been considered in the same way.

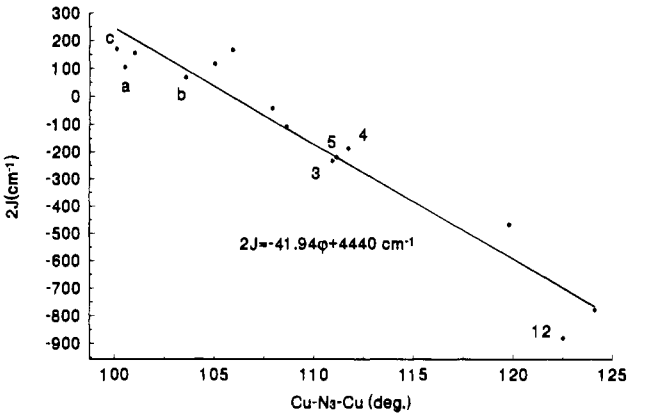

Figure 9. Plot of $2J$ (cm^{-1}) versus Cu−N_3−Cu bridge angle for the known di-μ_2-1,1-azide-bridged dinuclear copper(II) complexes and those involving one μ_2-1,1-azide and a diazine or hydroxide as a second bridge. The unidentified points are from ref 5.

It is apparent since a substantial improvement in the data fits for **1**−**5** occurs when significant negative Θ corrections are employed, which effectively corresponds to a situation involving two intramolecular antiferromagnetic exchange pathways, that there may be a way to differentiate or partition the exchange in weakly to moderately coupled, asymmetric complexes of this sort. The complex $[Cu_2(PAP)(\mu_2\text{-}N_3)(N_3)_3]\cdot CH_3OH.0.5H_2O$,[19] which appears to be structurally similar to **1** and **3**, with a single μ_2-1,1-azide bridge, has a $T(\chi_{max})$ of ≈75 K and will not fit the Bleaney−Bowers equation at all unless a very large negative Θ is used ($g = 2.243(4)$, $-2J = 48.6(7)$ cm^{-1}, $\Theta = -172(2)$ K, $10^2R = 0.61$). However, at this juncture no such equation is forthcoming, and the magnetic analysis in this paper has been carried out by assuming just one singlet−triplet energy level scheme and just one exchange integral.

The current study provides additional examples of μ_2-1,1-azide-bridged dicopper complexes which fall in the antiferromagnetic realm, with bridge angles in excess of 108°. For **1**, **3**−**5**, and **12** it is reasonable to assume that the azide propagates antiferromagnetic coupling. Figure 9 shows a plot of the existing diazine/azide complexes already published,[5] the new ones described in this paper (compound **1** has been excluded because no reasonable data fit to eq 1 was obtained with small Θ values), and also two di-μ_2-1,1-azide complexes (**a**, **b**) from the early literature described by Kahn.[3,4] What is remarkable is the fact that, despite some spread in the data, a reasonable linear trend is apparent. In our earlier paper[5] most of the azide-bridged complexes involved a second, diazine bridge, which acted complimentarily in the antiferromagnetic realm. **c** is a di-μ_2-1,1-azide complex, $[Cu_2(DMPTD)(\mu_2\text{-}N_3)_2(N_3)_2]$ (DMPTD = 2,5-bis-(pyridylmethyl)thio)thiadiazole).[5] The observed trend can be rationalized by assuming that the diazine bridge acts antiferromagnetically, but in a minor and roughly constant way in comparison with azide, and so the overall trend expresses the changes associated with the azide as its angle changes. **a**−**c** are reasonably placed close to the best fit line in the ferromagnetic realm, but two ferromagnetic complexes with equatorial

(24) Nishida, Y.; Takeuchi, M.; Takahashi, K.; Kida, S. *Chem. Lett.* **1985**, 631.
(25) Nishida, Y.; Kida, S. *J. Chem. Soc.* **1986**, 2633.
(26) McKee, V.; Zvagulis, M.; Reed, C. A. *Inorg. Chem.* **1985**, *24*, 2914.
(27) Benzekri, A.; Dubourdeaux, Latour, J.-M.; Laugier, J.; Rey, P. *Inorg. Chem.* **1988**, *27*, 3110.
(28) Benzekri, A.; Dubourdeaux, Latour, J.-M.; Rey, P.; Laugier, J. *J. Chem. Soc., Dalton Trans.* **1991**, 3359.
(29) Karlin K. D.; Cohen, B. I.; Hayes, J. C.; Farooq, A.; Zubieta, J. *Inorg. Chem.* **1987**, *26*, 147.
(30) Karlin, K. D.; Farooq, A.; Hayes, J. C.; Cohen, B. I.; Rowe, T. M.; Sinn, E.; Zubieta, J. *Inorg. Chem.* **1987**, *26*, 1271.
(31) Mallah, T.; Kahn, O.; Gouteron, J.; Jeannin, S.; Jeannin, Y.; O'Connor C. J. *Inorg. Chem.* **1987**, *26*, 1375.
(32) Kahn, O.; Charlot, M. F. *Nouv. J. Chem.* **1980**, *4*, 567.
(33) Mandal, S. K.; Thompson, L. K.; Gabe, E. J.; Charland, J.-P.; Lee, F. L. *Inorg. Chem.* **1988**, *27*, 855.
(34) Tandon, S. S.; Thompson, L. K.; Hynes, R. C. *Inorg. Chem.* **1992**, *31*, 2210.

($d_{x^2-y^2}$ ground state copper) combinations of μ_2-1,1-azide and μ_2-hydroxide bridges do not fit the line (not shown in Figure 9) and are displaced downward significantly (Cu−N_3−Cu 95.7°, Cu−OH−Cu 102.5°, and $2J$ = 200 cm^{-1} [35] for $[Cu_2L_2(OH)(N_3)](ClO_4)_2$ (L = 1,4,7-trimethyl-1,4,7-triazacyclononane) Cu−N_3−Cu 93.0°, Cu−OH−Cu 103.0°, and $2J$ = 44 cm^{-1} [36]). Using Hatfield's correlation for dihydroxo-bridged dicopper(II) complexes,[1] substantial antiferromagnetic terms would be expected for these compounds, associated with the hydroxide bridges, and so weaker ferromagnetic coupling would be anticipated. The equation of the best fit line (eq 2) does not

$$2J = -41.94\Phi + 4440\ cm^{-1} \quad (2)$$

take into account the presence of the diazine bridge, and the calculated azide bridge angle (Φ_0) at which the net exchange is zero (105.3°) is slightly smaller than that estimated in the previous study[5] but is consistent with extended Hückel calculations[2] for the μ_2-1,1-azide bridge. Preliminary results with μ_2-1,1-azide-bridged dinickel systems indicate that an antiferromagnetic realm for nickel azide complexes also exists.[37]

Conclusion

The antiferromagnetic realm for the μ_2-1,1-azide bridge has been further established by the synthesis and study of additional examples of dicopper(II) complexes with azide bridge angles exceeding 108°.

Acknowledgment. We thank the Natural Sciences and Engineering Research Council of Canada for financial support for this study and Dr. J. N. Bridson for X-ray structural analyses.

Supplementary Material Available: Tables listing detailed crystallographic data, hydrogen atom positional parameters, anisotropic thermal parameters, bond lengths and angles, and least-squares planes (53 pages). Ordering information is given on any current masthead page.

IC941160C

(35) Kahn, O.; Sikorav, S.; Gouteron, J.; Jeannin, S.; Jeannin, Y. *Inorg. Chem.* **1983**, *22*, 2877.
(36) Chaudhuri, P. Personal communication.
(37) Sheppard, C. L.; Thompson, L. K. Unpublished results.